DECOVALEX 2023 Task D – Interim Report from SNL

SNL Team / Authors

Carlos Jove-Colon
Carlos M Lopez
Kris Kuhlman

1. Simulation code

Computer simulations were done using the code PFLOTRAN, a massively parallel subsurface flow and reactive-transport code for hydrogeochemical applications [1]. The code leverages thermal, hydraulic, and chemical capabilities, with several input modes that allow for single- and multiphase flow in variably saturated porous media and reactive-transport simulations.

The 1-D model uses PFLOTRAN's General Mode for thermal and hydraulic calculations of two-phase (liquid/gas) flow and no reactive transport (i.e., no chemical interactions). Thermal conductivity can be specified to be constant or as a function of liquid saturation. Permeability in PFLOTRAN can be constrained to be constant and isotropic through porous domain; however, the simulator can also account for changes in permeability as a function of porosity. Additionally, anisotropic permeabilities can be specified as an input constraint. The water retention curve and relative permeabilities are computed as a function of liquid saturation.

2. PFLOTRAN 1-D Model Setup and Results

S1-3

The S1-3 experiment is described elsewhere in this report. The simulated 1-D isothermal Kunigel V1 bentonite and sand domain is 50 cells in Z, with each cell 1 mm tall, for a total 50 mm sample height (see **Fig. 1**). The water inlet was modeled as a saturation-driven fluid transport into porous bentonite and sand from a large liquid reservoir at the bottom of the sample. This reservoir is implemented as an inflow boundary condition on the bottom face of the sample. The air outlet was modeled via an outflow boundary condition on the top face of the sample. The pressure condition was atmospheric. All simulations were conducted at 25 °C.

These simulations do not account for chemical interactions between pore solution and bentonite. That is, the potential for chemical reactions between bentonite and pore fluids that could lead to swelling are not considered as part of the bentonite saturation mechanism. Porosity is held constant at 32.8%. As such, a suitable mechanism that could control time-dependent saturation as well as account for the different behaviors of the two fluids was needed. To this end, we implemented a heterogeneous permeability distribution that was treated as an input variable and was constrained to fit the experimental data. The bentonite block was divided into two regions having different isotropic permeability. The size and permeabilities of these regions depend on

the wetting fluid being modeled, which is either deionized water (DW) or groundwater (GW). These regions and permeabilities are depicted in **Fig. 1** and listed in **Table 1**.

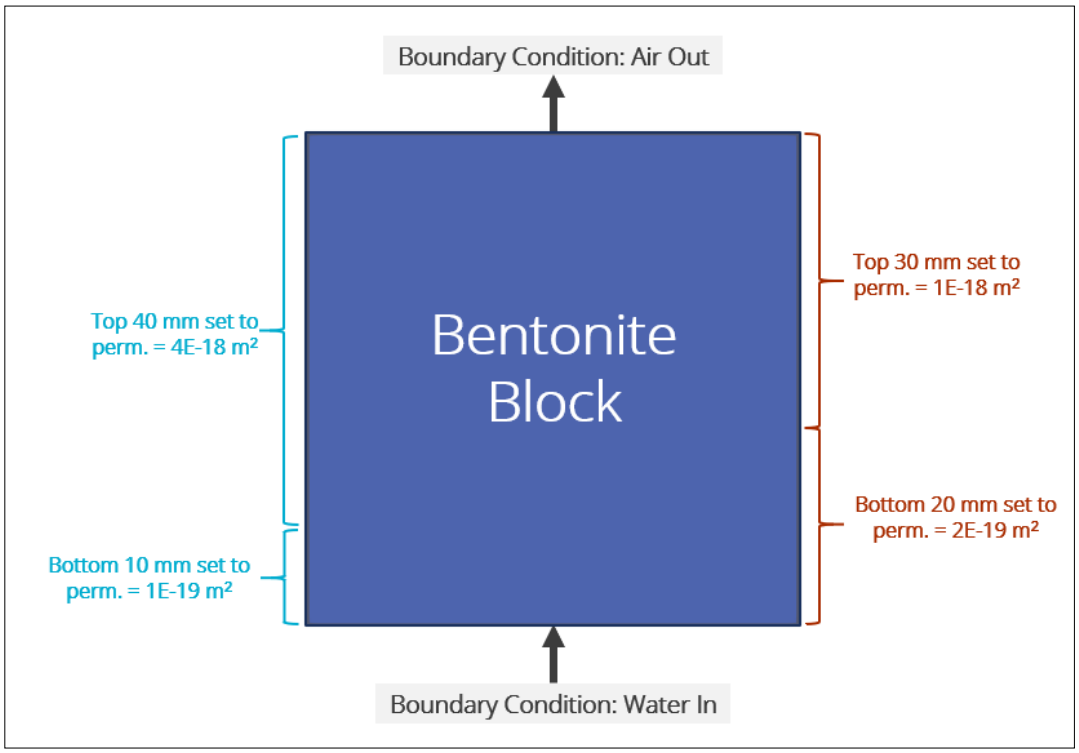

Fig. 1. Schematic illustration of the PFLOTRAN 1-D simulation domain and boundary conditions for experiment S1-3. Permeabilities/regions for the distilled water case are depicted in blue (left) whereas those corresponding to the groundwater case are depicted in red (right). "Perm." refers to isotropic permeability.

Table 1. Case-dependent regional permeabilities.

Case	Region	Height (mm)	Permeability (m^2)
DW Case	Top	40	4E-18
	Bottom	10	1E-19
GW Case	Top	30	1E-18
	Bottom	20	2E-19

Two different initial saturation conditions were tested for both the GW and DW cases: heterogeneous and homogeneous. In the heterogeneous case, the bentonite was divided into ten regions where initial liquid saturation was set to represent temporal data obtained from the DW experiment (**Table 2**). In the homogeneous case, the entire block was assigned an initial liquid saturation of 33.4% which is the average of the values used for the heterogeneous case. The

saturation profiles are visualized in **Figure 2**. In all cases, a liquid residual saturation of 15% and a gas residual saturation of 0.1% were used. The van Genuchten[2] saturation function implemented in PFLOTRAN[1] was used with parameter values of M = 0.275 and α = 5.1e-7. A limitation of the model is that a saturation above 100% cannot be predicted, even though the experimental data indicates >100% saturation at later times. The relative permeability function is based on a combined Mualem-van Genuchten formulation[1,3].

Table 2. Initial liquid saturations assigned to regions in heterogeneous saturation tests.

Region (Distance from the bottom of the sample)	Initial Liquid Saturation
0 mm - 5 mm	34%
5 mm - 10 mm	30%
10 mm - 15 mm	37%
15 mm - 20 mm	36%
20 mm - 25 mm	28%
25 mm - 30 mm	33%
30 mm - 35 mm	30%
35 mm - 40 mm	36%
40 mm - 45 mm	38%
45 mm - 50 mm	34%

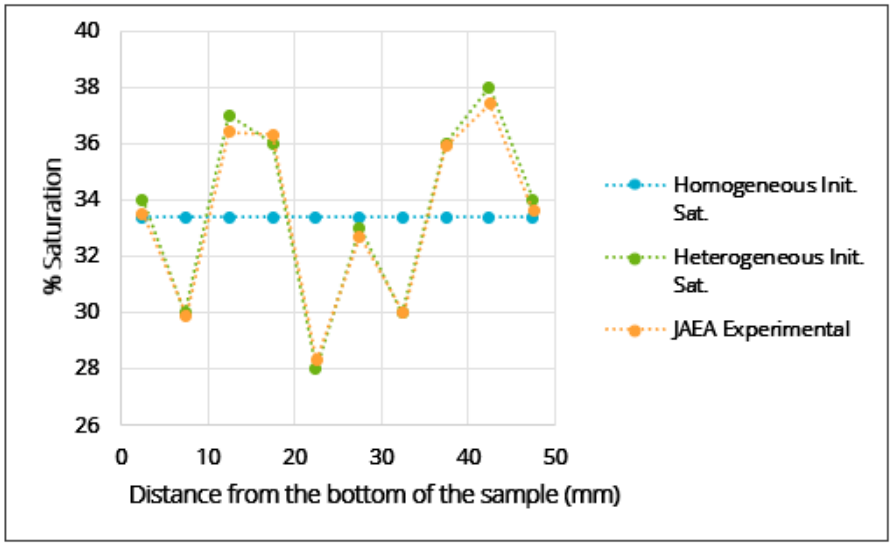

Figure 2. Initial saturation profiles for the homogeneous and heterogeneous cases.

The results of the DW tests are summarized in **Figure 3**. The PFLOTRAN 1-D model is successful in representing the saturation profiles of the S1-3 experiment in Kunigel V1 bentonite

and sand, for both the DW and GW cases and with both heterogeneous and homogenous initial saturation conditions.

After 1 day of saturation time, the profiles of the PFLOTRAN model are similar to that of the experimental data, except for a discrepancy at 22.5 mm from the bottom of the sample. At 10 and 15 days, the simulations tend to overpredict saturation in the region between 10 and 40 mm from the bottom of the sample. However, this is improved at 30 days with the only point of notable difference being the region near the top of the sample.

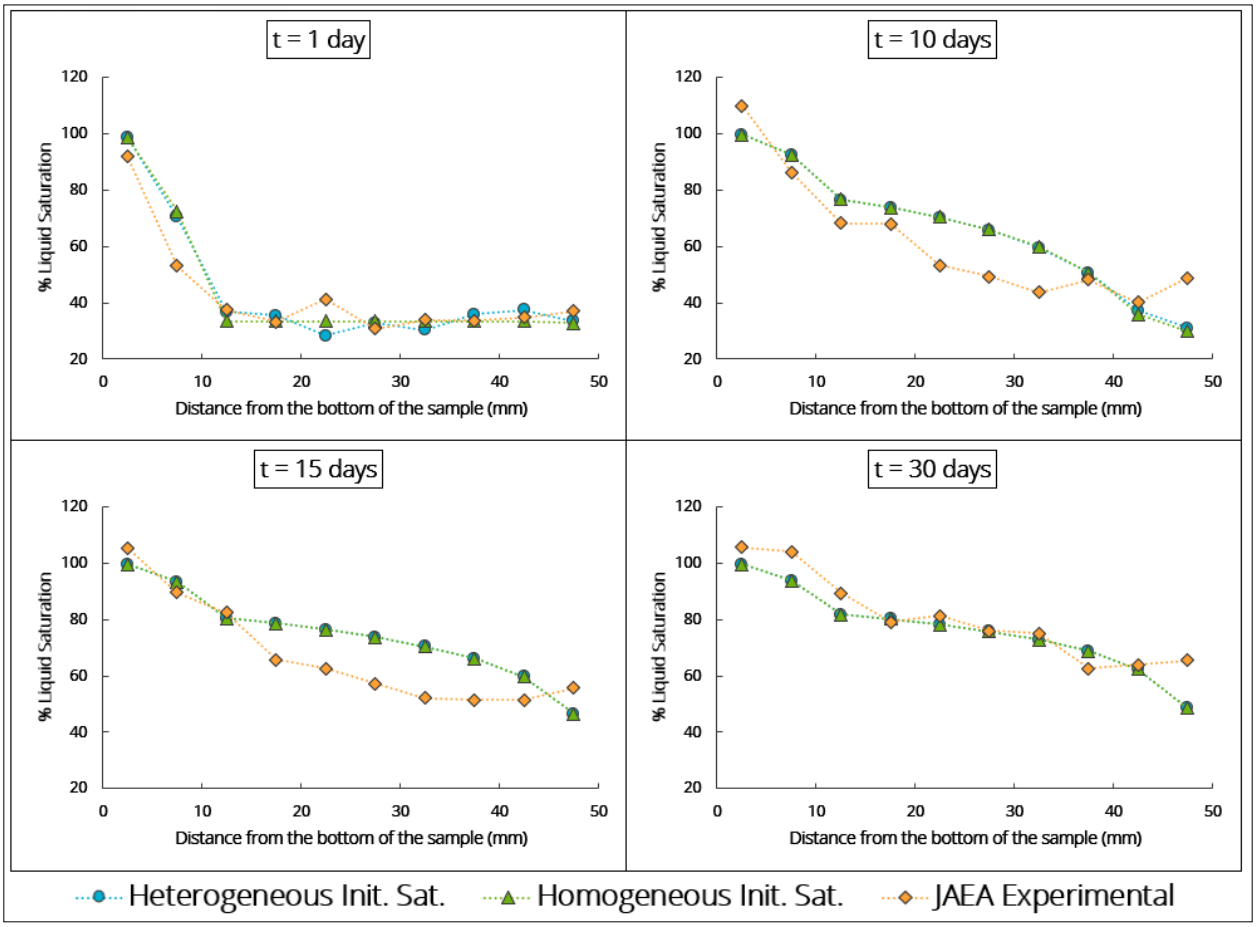

Figure 3. Saturation over distance profiles at after 1, 10, 15, and 30 days of saturation time, for the DW case. (Note: In the 10-, 15-, and 30-day plots, the plotted results for the homogeneous and heterogeneous cases are nearly identical.)

The results of the GW case are summarized in **Figure 4**. As with the DW case, after 1 day of saturation time, the profiles of the PFLOTRAN simulations are similar to that of the experimental data even when the model noticeably overpredicts saturation at 7.5 mm from the bottom of the sample. Discrepancies at 10 and 14 days persist as the PFLOTRAN simulations overestimate saturation closer to the bottom of the sample and underestimate closer to the top of the sample. As before, differences between simulations and experimental data are reduced at 30 days with the only notable departures occurring near the top and bottom of the sample.

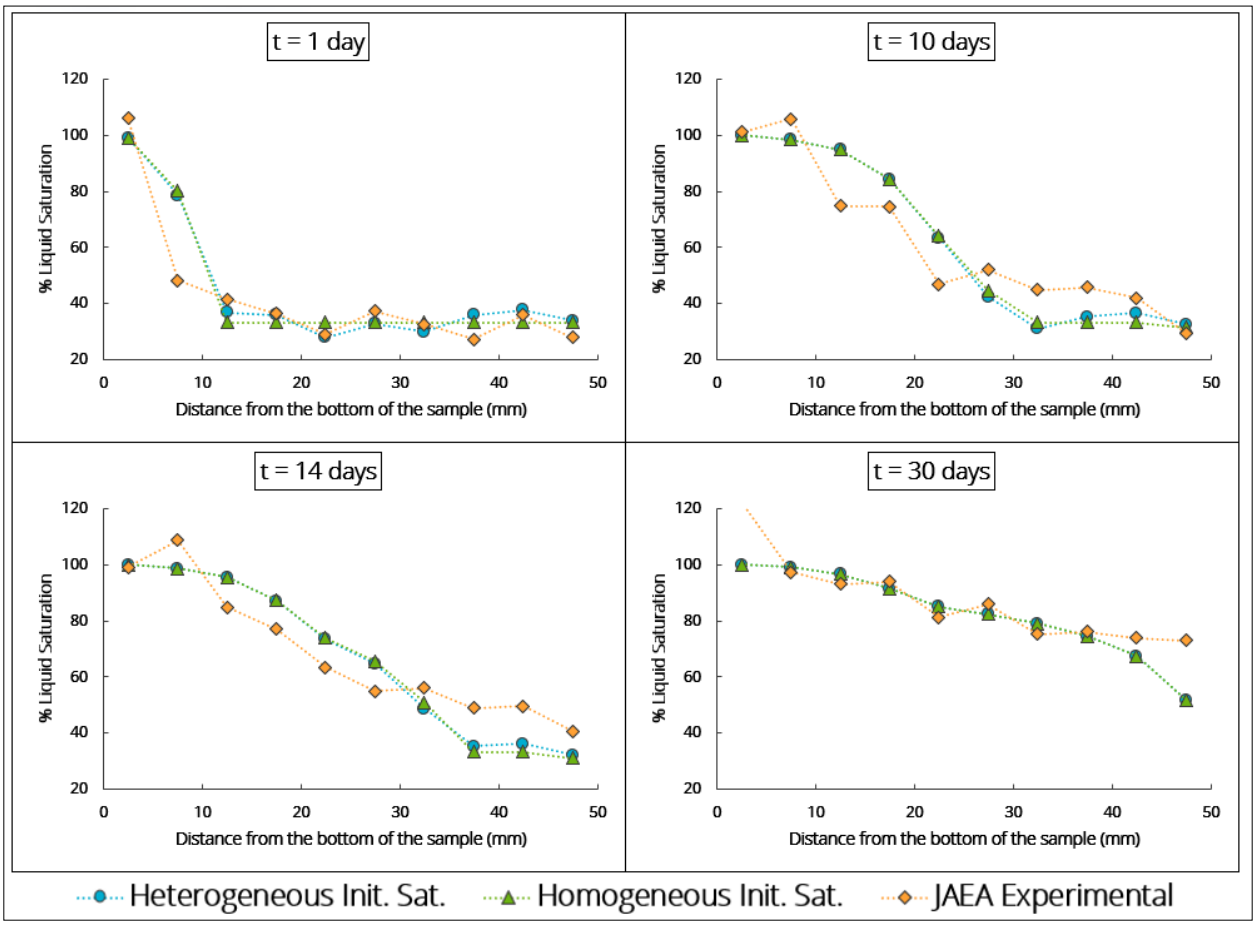

Figure 4. Saturation over distance profiles at after 1, 10, 14, and 30 days of saturation time, for the GW case. (Note: In the 30-day plot, the homogeneous and heterogeneous cases plot nearly identically.)

Initial saturation profiles (homogeneous vs. heterogeneous) primarily affect predicted saturation profiles at early times. That is, the difference between model predictions made based on homogeneous vs. heterogeneous initial saturation decreases as simulated time increases. **Figure 5** shows the largest difference among the homogeneous vs. heterogeneous initial saturation cases at any given time (arbitrary location along the sample). At any given time, the difference in predicted saturation between the two initial saturation profiles decreases and eventually drops well below 1%. Discrepancies are smaller at earlier times in the DW than in the GW simulations.

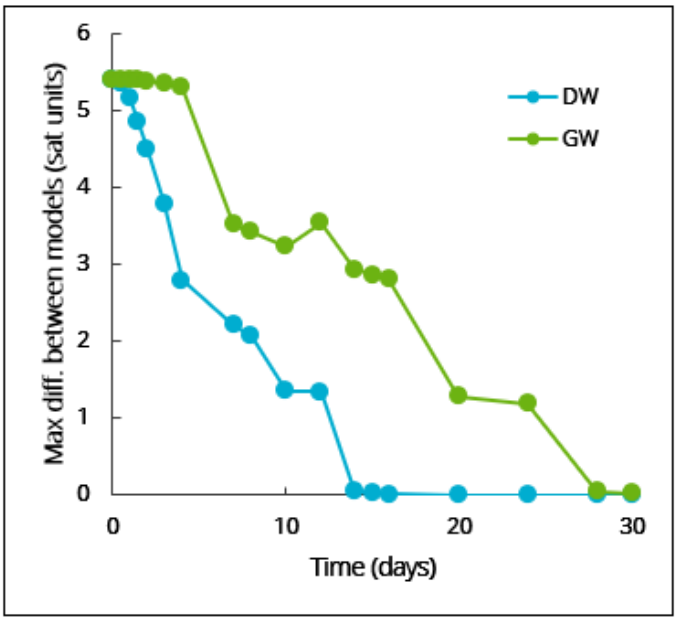

Figure 5. Maximum observed differences in predicted % (point) saturation at any sample location with time between simulations with homogeneous and heterogeneous initial saturation conditions.

S1-4

The modeling results described in this section for Experiment S1-4 are preliminary and as such are considered work in progress. The S1-4 experiment is described elsewhere in this report. The modeled domain is 100 cells in Z, with each cell 1 mm tall, for a total 100 mm sample height. The 1-D problem was modeled as a closed system saturation-driven transport. That is, all boundaries were constrained to have no mass or thermal fluxes. As with S1-3, the adopted saturation function was the van Genuchten formulation with M = 0.275 and α = 5.1e-7. Pressure is allowed to change with gradients in temperature across the simulated domain.

Key to this problem was the development of a temperature gradient along the vertical length of sample. The temperature gradient developed as a result of constant temperature boundary conditions on the top (30 °C) and the bottom (70 °C) faces of the sample. The considered thermal conductivity values for dried and wet bentonite having a dry density of 1.8 g/cm^3 are 0.798 and 1.94 W/m-K, respectively. The thermal conductivity values were provided by the JAEA to the task members. All other boundaries were set to have zero thermal flux. The bentonite domain had an initial condition of T = 25 °C. See **Fig. 6**.

The bentonite domain has initial uniform liquid saturation of 32%. This is approximated from an estimated water content of 10.5% and a constant porosity of 32.8% using the following equation (**Eq. 1**):

$$\frac{\%\ Water\ Content}{\%\ Porosity} * 100\% = \%\ Liquid\ Saturation \quad (1)$$

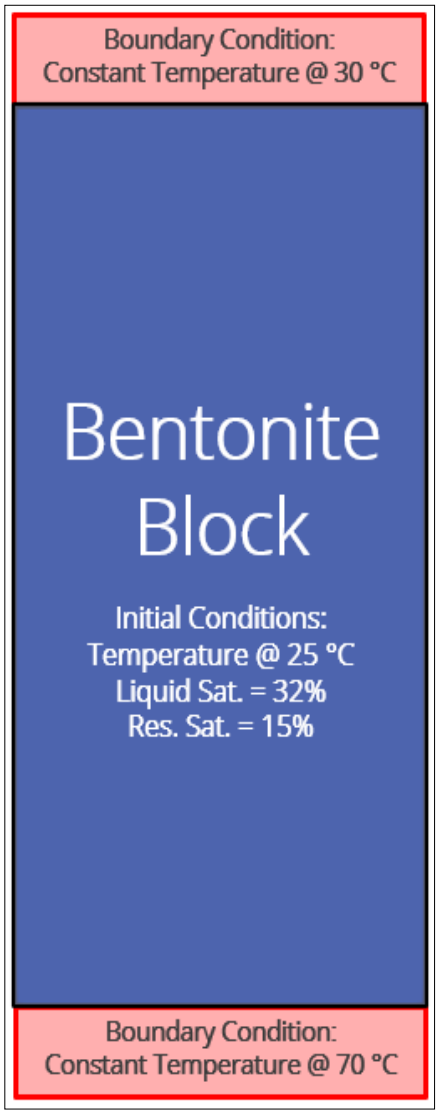

Fig. 6. Schematic illustration of the non-isothermal PFLOTRAN 1-D simulation domain and boundary conditions for the experiment S1-4.

Water content will be assessed as an equivalent % liquid saturation as the latter is a PFLOTRAN output. The liquid residual saturation was set to 15%.

As with S1-3, these simulations do not account for the chemical and mechanical processes (i.e., bentonite swelling) occurring in the sample during the saturation experiment. Permeability was again treated as an adjustable input to fit experimental data. However, in this case, permeability was treated as homogeneous throughout the whole sample domain. An initial permeability value of 5e-18 m^2 was adopted. Saturation profiles corresponding to permeabilities of 1e-18 m^2 and 1e-17 m^2 were also evaluated.

The predicted temperature profile across the sample is approximately linear as seen in **Figure 7**. However, as the simulation progresses, slight deviations from linearity are introduced within the bottom region of the sample.

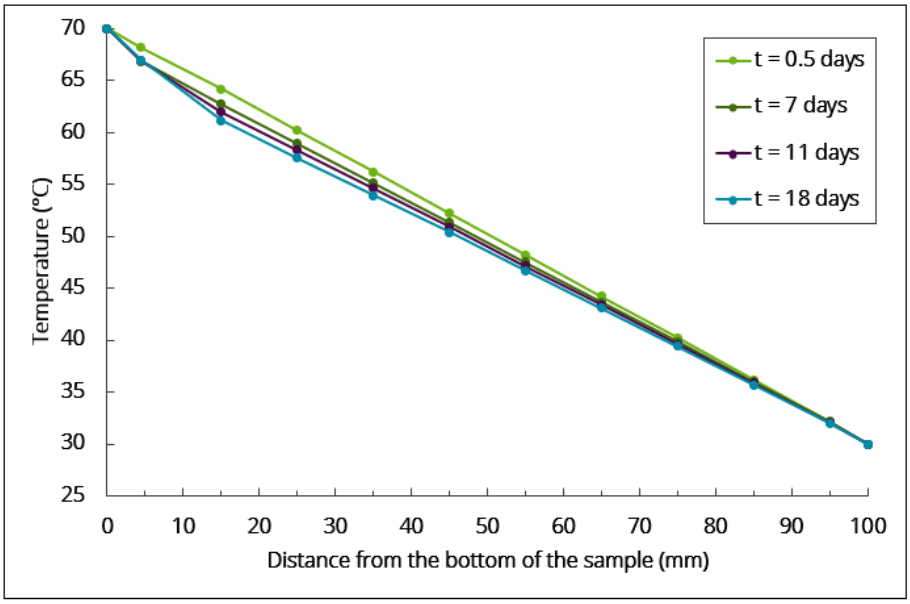

Figure 7. Temperature profile in the PFLOTRAN model of Experiment S1-4 where permeability was set to 5e-18 m^2.

PFLOTRAN simulations have not yet been able to closely replicate the trends in liquid saturation observed in the S1-4 experimental data. **Figure 8** shows that at high enough permeabilities saturation drops below the 15% residual value (all the way down to 0%) for cells close to the 70°C boundary. Model predictions of liquid saturation at the top of the sample tend to underpredict the experimental data. The exception to this is at the highest permeability case where the simulated saturation is higher than the experimental data. **Figure 9** shows the liquid and gas pressures that result in the model with permeability equals to 5e-18 m^2. Current work is focused on evaluating the non-isothermal effects of liquid and gas pressure changes through the bentonite domain. Also, parameter sensitivity evaluations on the van Genuchten and Mualem-van Genuchten formulations on predicted saturation and relative permeabilities are currently under way.

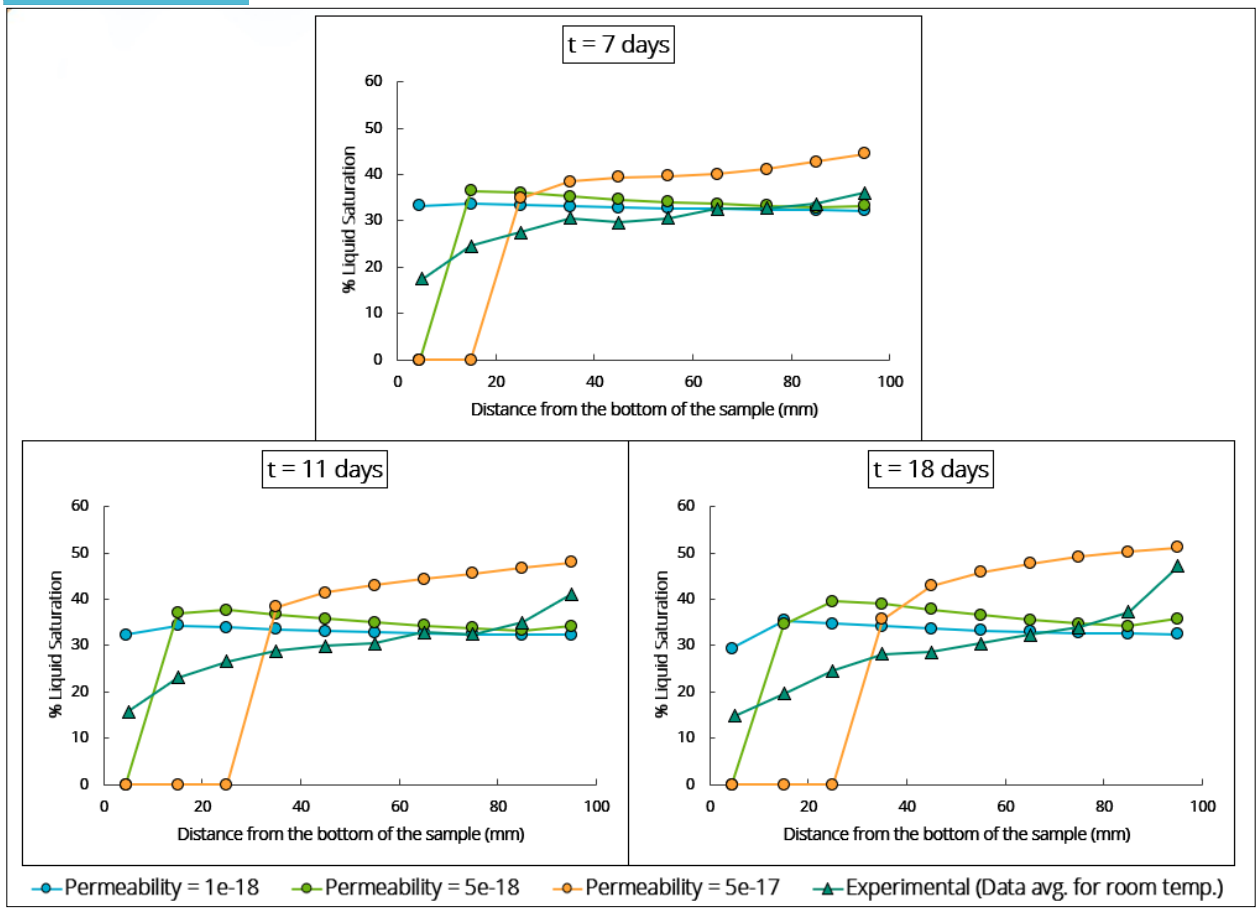

Figure 8. Saturation profiles for PFLOTRAN simulations of Experiment S1-4 at three different permeabilities, compared against the average of the experimental data for samples initially at room temperature.

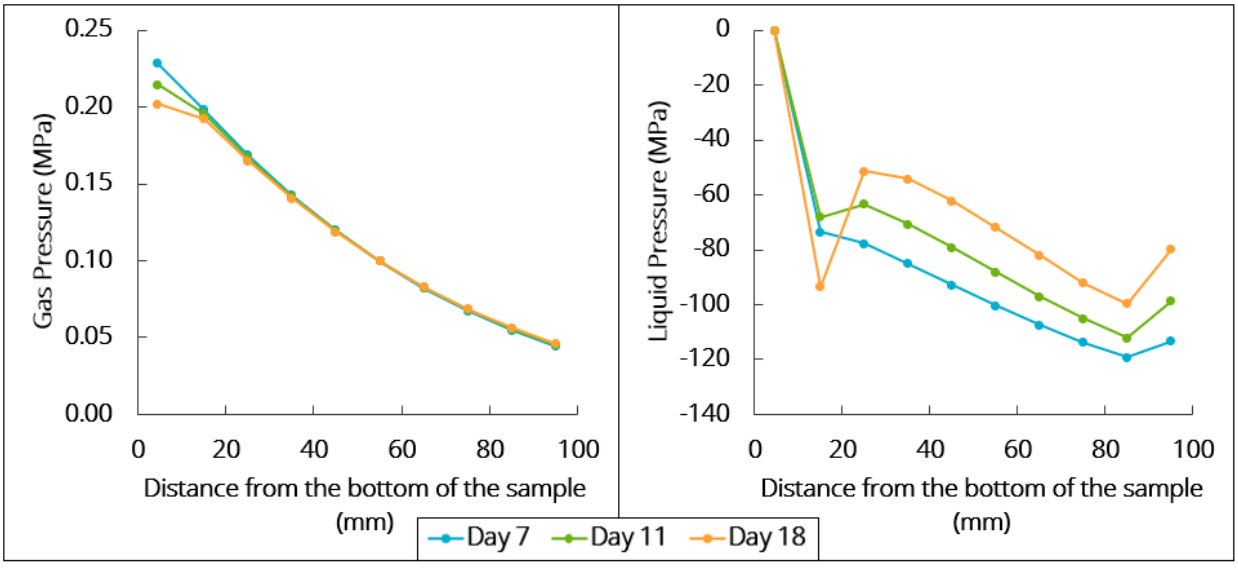

Figure 9. Gas (left) and liquid (right) pressure profiles in the PFLOTRAN model of Experiment S1-4 where permeability was set to 5e-18 m^2.

3 Concluding Remarks

The capability of a 1-D PFLOTRAN model to simulate the S1-3 bentonite saturation experiment has been demonstrated and validated against experimental data. Work remains to be done to refine 1-D PFLOTRAN simulations of the experiment S1-4 which include evaluation of parameter sensitivities on the prediction of material saturation and relative permeabilities. This and further testing of PFLOTRAN capabilities will be done as part of DECOVALEX 2023 Task D contributions by the SNL team in the coming months.

Disclaimer

Sandia National Laboratories is a multimission laboratory managed and operated by National Technology and Engineering Solutions of Sandia LLC, a wholly owned subsidiary of Honeywell International Inc. for the U.S. Department of Energy's National Nuclear Security Administration under contract DE-NA0003525. SAND####-####

References

[1] Lichtner, P.C., Hammond, G.E., et al. (2019) PFLOTRAN user manual: A massively parallel reactive flow and transport model for describing surface and subsurface processes. Los Alamos National Lab. (LANL), Los Alamos, NM (United States); http://documentation.pflotran.org.

[2] van Genuchten, M.T. (1980) A Closed-form Equation for Predicting the Hydraulic Conductivity of Unsaturated Soils. Soil Sci Soc Am J 44, 892-898.

[3] Mualem, Y. (1976) A new model for predicting the hydraulic conductivity of unsaturated porous media. Water resources research 12, 513-522.